Macromolecules

Article

pubs.acs.org/Macromolecules

RAFT-based Polystyrene and Polyacrylate Melts under Thermal and Mechanical Stress

Ozcan Altintas,[†,‡,§] Kamran Riazi,[‡] Richmond Lee,[⊥] Ching Y. Lin,[⊥] Michelle L. Coote,[⊥] Manfred Wilhelm,[‡,*] and Christopher Barner-Kowollik[†,§,*]

[†]Preparative Macromolecular Chemistry, Institut für Technische Chemie und Polymerchemie, Karlsruhe Institute of Technology (KIT), Engesserstrasse 18, 76128 Karlsruhe, Germany

[‡]Polymeric Materials, Institut für Technische Chemie und Polymerchemie, Karlsruhe Institute of Technology (KIT), Engesserstrasse 18, 76128 Karlsruhe, Germany

[§]Institut für Biologische Grenzflächen, Karlsruhe Institute of Technology (KIT), Hermann-von-Helmholtz-Platz 1, 76344 Eggenstein-Leopoldshafen, Germany

[⊥]ARC Centre of Excellence for Free-Radical Chemistry and Biotechnology, Research School of Chemistry, Australian National University, Canberra, ACT 0200, Australia

Supporting Information

ABSTRACT: Although controlled/living radical polymerization processes have significantly facilitated the synthesis of well-defined low polydispersity polymers with specific functionalities, a detailed and systematic knowledge of the thermal stability of the products—highly important for most industrial processes—is not available. Linear polystyrene (PS) carrying a trithiocarbonate mid-chain functionality (thus emulating the structure of the Z-group approach via reversible addition−fragmentation chain transfer (RAFT) based macromolecular architectures) with various chain lengths (20 kDa $\leq M_{n,SEC} \leq$ 150 kDa, 1.27 $\leq Đ = M_w/M_n \leq$ 1.72) and chain-end functionality were synthesized via RAFT polymerization. The thermal stability behavior of the polymers was studied at temperatures ranging from 100 to 200 °C for up to 504 h (3 weeks). The thermally treated polymers were analyzed via size exclusion chromatography (SEC) to obtain the dependence of the polymer molecular weight distribution on time at a specific temperature under air or inert atmospheres. Cleavage rate coefficients of the mid-chain functional polymers in inert atmosphere were deduced as a function of temperature, resulting in activation parameters for two disparate M_n starting materials (E_a = 115 ± 4 kJ·mol^{-1}, A = 0.85 × 10^9 ± 1 × 10^9 s^{-1}, $M_{n,SEC}$ = 21 kDa and E_a = 116 ± 4 kJ·mol^{-1}, A = 6.24 × 10^9 ± 1 × 10^9 s^{-1}, $M_{n,SEC}$ = 102 kDa). Interestingly, the degradation proceeds significantly faster with increasing chain length, an observation possibly associated with entropic effects. The degradation mechanism was explored in detail via SEC−ESI−MS for acrylate based polymers and theoretical calculations suggesting a Chugaev-type cleavage process. Processing of the RAFT polymers via small scale extrusion as well as a rheological assessment at variable temperatures allowed a correlation of the processing conditions with the thermal degradation properties of the polystyrenes and polyacrylates in the melt.

INTRODUCTION

During the past few decades, the academic use of controlled/living radical polymerization (CLRP) techniques for the synthesis of well-defined narrow polydispersity polymers has rapidly increased due to the variety of applicable monomers and the more tolerant experimental conditions than living ionic polymerization routes.[1] However, the increasing use of CLRP methods for the design of complex macromolecular architectures requires detailed knowledge regarding the thermal and mechanical stability of the resulting polymeric materials under industrially relevant processing conditions to foster further use of these new synthetic possibilities.[2]

Received: August 21, 2013
Revised: September 20, 2013
Published: October 7, 2013

Scheme 1. General Strategy Followed in the Current Study for Understanding the Thermal and Mechanical Stability of RAFT Polymer Melts, Carrying a Trithiocarbonate Moiety in the Mid-Chain or Chain-End Position

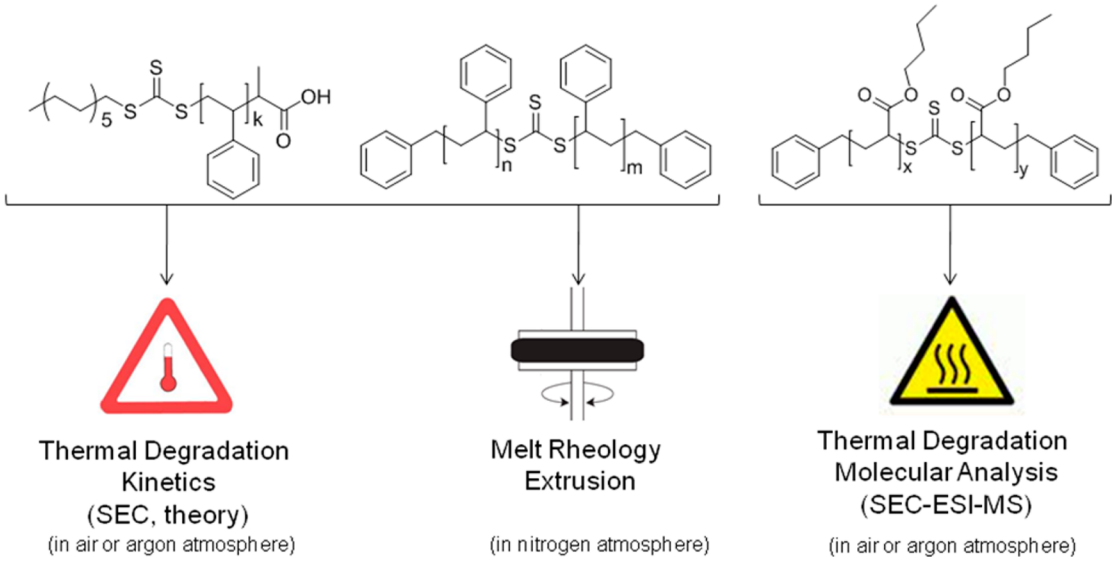

A transition metal mediated controlled/living radical polymerization process such as atom transfer radical polymerization (ATRP),[3−6] the nitroxide-mediated radical polymerization (NMP),[7,8] and reversible addition−fragmentation chain transfer (RAFT) polymerization[9−12] are currently the most applied CLRP processes. In particular, the RAFT polymerization has been proven to be highly versatile and efficient (e.g., various types of monomers, wide solvent selection, etc.), allowing for fine control over variable molecular architectures as well as the molecular weight and dispersity of the prepared synthetic polymers, while being highly tolerant to functional monomers under nondemanding reaction conditions with respect to, e.g., solvent, functional groups, and temperature.[13] Importantly, the RAFT process proceeds under identical polymerization conditions as conventional free radical polymerization, in which a conventional chain transfer agent is substituted by a RAFT agent. The adaptation of the RAFT process to large scale polymer production thus requires very little change from established industrial setups.[14,15]

To generate complex macromolecular architectures via the RAFT process, there are two principal approaches: attachment of the RAFT agent's Z-group or leaving R-group to a central linking core (see Scheme S1 in the Supporting Information).[16] The Z-group design is typically preferred over the R-group approach, as it avoids the formation of higher-order coupling products. In the Z-group approach, the RAFT agent is covalently attached to the structural framework of the core and thus the core never carries radical functions excluding the possibility of core−core couplings.[16] In contrast—in ATRP and NMP—the core carries the radical species by default and thus core−core coupling reactions occur, which can only be minimized by carefully selecting the reaction conditions (e.g., low conversions, low radical fluxes, or the use of a rapidly propagating monomer).[17] As a consequence, the design of complex macromolecular architectures preferentially proceeds via the Z-group approach, as it provides the ability to synthesize highly pure and well-defined polymers up to high monomer-to-polymer conversions without cross coupling products.[17] However, a potential disadvantage of the Z-group approach is the fact that all chains are tethered to the central core via a thiocarbonylthio linkage, which is a potentially weak connection when processing Z-group-based RAFT-designed polymers.

Thiocarbonylthio compounds play a central role in RAFT processes and macromolecular architecture design.[18,19] Although the synthesis of RAFT polymers as well as polymers with variable conjugation units with varied topology has been widely employed,[20−24] there is no systematic knowledge regarding the stability of the generated polymers with regard to their thiocarbonylthio functionality at elevated temperatures under polymer processing conditions. One of the most important aspects for processing and the use of polymers on an industrial scale is the knowledge of their stability in the melt under extrusion conditions and the associated typical shear rates and temperatures.[25,26]

In the present study, we carefully investigate the stability of linear RAFT polystyrene and polyacrylate melts that carry a mid-chain thiocarbonylthio function emulating a Z-group linkage under thermal and mechanical stress with the aim of developing an encompassing mechanistic, kinetic and rheological image of the degradation process. Well-defined linear polystyrenes (PS) carrying a trithiocarbonate functionality in the middle of the polymer chain with various chain lengths (20 kDa $\leq M_{n,SEC} \leq$ 150 kDa, 1.27 $\leq Đ \leq$ 1.72) have thus been prepared. In addition—and for comparison and as reference—a polymer featuring a trithiocarbonate end group ($M_{n,SEC}$ = 139.2 kDa; $Đ$ = 1.68) as well as anionically prepared polystyrenes ($M_{n,SEC}$ = 267 kDa; $Đ$ = 1.11 and $M_{n,SEC}$ = 70.9 kDa; $Đ$ = 1.04) were employed. The thermal stability of RAFT-functionalized polystyrenes was mainly studied at elevated temperatures and a detailed kinetic investigation of the degradation of the RAFT polymers was carried out at variable temperatures under an inert atmosphere as well as under air. High-level *ab initio* molecular orbital theory calculations were undertaken to help interpret the experimental results. To explore the mechanism of degradation associated with the mid-chain RAFT group, linear poly(*n*-butyl acrylate) (P*n*BA)[27] with a midterm position of the trithiocarbonyl functionality in the polymer chain as in the polystyrenes was synthesized via RAFT polymerization. The P*n*BA polymers were subjected to identical thermal degradation

dx.doi.org/10.1021/ma401749h | *Macromolecules* 2013, 46, 8079−8091

conditions as the polystyrenes prior to ESI–MS analysis. The choice of P*n*BA for this propose is based on its much better ionizability during ESI and the fact that trithiocarbonate mid-chain functional polymers can be prepared with similar ease as polystyrenes via the RAFT process. Finally, the prepared polymers were subjected to extrusion experiments and a rheological assessment to correlate the obtained kinetic data with actual processing conditions. Additionally, rheological assessments are very sensitive due to the approximately cubic dependence of the viscosity on molecular weight, $\eta \sim M_n^{3.4}$, as shown by reptation theory.[28,32,33,53] Thus, a systematic correlation between Z-group architecture RAFT polymers, their chain length and the processing conditions is achieved (Scheme 1).

EXPERIMENTAL SECTION

All manipulations of air-sensitive materials were performed under the rigorous exclusion of oxygen and moisture in Schlenk-type glassware on a dual manifold Schlenk line interfaced to a high vacuum line (10^{-5} bar).

Materials. Styrene (99% extra pure, Acros) and *n*-butyl acrylate (99% extra pure, Acros) were destabilized by passing through a basic alumina column and stored at −19 °C. 2,2′-Azobis(2-methylpropionitrile) (AIBN, Sigma-Aldrich) was recrystallized twice from methanol (MeOH, VWR) and stored at −19 °C. Toluene (extra dry over molecular sieve, 99.85%, Acros) was used as received. 2-((dodecylsulfanyl)carbonothioyl)sulfanyl propanoic acid (DoPAT) and dibenzyl trithiocarbonate (DBTTC) were obtained from Orica Pty Ltd., Melbourne, Australia as a donation. The two linear polystyrene homopolymers (**4a**, $M_{n,SEC}$ = 267 kDa, $Đ$ =1.11 and **4b**, $M_{n,SEC}$ = 70.3 kDa, $Đ$ =1.04) were prepared via anionic polymerization and serve as reference materials.

Instrumentation. *Size Exclusion Chromatography.* Size exclusion chromatography (SEC) measurements were performed on a Polymer Laboratories PL-SEC 50 Plus Integrated System, comprising an autosampler, a PLgel 5 μm bead-size guard column (50 × 7.5 mm) followed by three PLgel 5 μm Mixed-C and one PLgel 3 μm Mixed-E columns (300 × 7.5 mm), and a differential refractive index (DRI) detector using tetrahydrofuran (THF) as the eluent at 40 °C with a flow rate of 1 mL min^{-1}. The SEC system was calibrated using both linear polystyrene standards ranging from 160 to 6 × 10^6 g mol^{-1}. Calculation of the molecular weight proceeded via the Mark–Houwink–Sakurada (MHS) parameters for polystyrene (PS)[29] in THF at 30 °C, i.e., K = 14.1 × 10^{-5} dL g^{-1}, α = 0.70. For poly(*n*-butyl acrylate),[30] the corresponding MHS parameters were employed: K = 12.2 × 10^{-5} dL g^{-1}, α = 0.70.

Size-Exclusion-Chromatography Electrospray Ionization-Mass Spectrometry (SEC–ESI–MS). Mass spectra were recorded on a LXQ mass spectrometer (ThermoFisher Scientific) equipped with an atmospheric pressure ionization source operating in the nebulizer-assisted electrospray mode. The instrument was calibrated in the m/z range 195–1822 using a standard containing caffeine, Met-Arg-Phe-Ala acetate (MRFA) and a mixture of fluorinated phosphazenes (Ultramark 1621, all from Aldrich). A constant spray voltage of 4.5 kV and a dimensionless sweep gas flow rate of 2 (approximately 3 L min^{-1}) and a dimensionless sheath gas flow rate of 12 (approximately 1 L min^{-1}) were applied. The capillary voltage, the tube lens offset voltage and the capillary temperature were set to 60 V, 110 V and 275 °C respectively. The solvent was a 3: 2 v/v mixture of THF: methanol with a polymer concentration of 0.2 mg mL^{-1}. The instrumental resolution of the employed experimental setup is ±0.1 Da.

For SEC–ESI–MS the LXQ was coupled to a Series 1200 HPLC system (Agilent) that consisted of a solvent degasser (G1322A), a binary pump (G1312A) and a high performance autosampler (G1367B), followed by a thermostated column compartment (G1316A). Separation was performed on two mixed bed SEC columns (Polymer Laboratories, Mesopore 250 × 4.6 mm, particle diameter 3 μm) with precolumn (Mesopore 50 × 4.6 μm) operating at 30 °C. THF at a flow rate of 0.3 mL min^{-1} was used as the eluent. The mass spectrometer was coupled to the column in parallel to an DRI detector (G1362A with SS420 × A/D) in a setup described previously.[31] A 0.27 μL min^{-1} aliquot of the eluent was directed through the RI detector and 30 mL min^{-1} infused into the electrospray source after postcolumn addition of a 0.1 mM solution of sodium iodide in methanol at 20 μL min^{-1} by a microflow HPLC syringe pump (Teledyne ISCO, Model 100DM). The polymer solutions with a concentration of 2 mg mL^{-1} were injected into the HPLC system.

Rheometry. The rheological characterization of the melt polymers was carried out under nitrogen atmosphere using on an ARES classic strain-controlled rotational rheometer equipped with a 1KFRTN1 torque transducer from TA Instruments. Small amplitude oscillatory shear (SAOS) measurements were conducted in the linear regime using a parallel plate geometry (13 mm, gap ≈1 mm) in the temperature range from 160 to 200 °C and the frequency range from $\omega/2\pi$ = 0.01 to 15 Hz at each temperature. To determine the linear viscoelastic region,[32,33] strain sweep experiments were performed before the frequency sweep tests via variable amplitude oscillatory shear. The instrument was equipped with two transducers covering the torque range from 2 × 10^{-6} to 0.2 Nm. A nitrogen atmosphere was kept during the heating using a forced convection oven from ambient temperature to test conditions. All dynamic measurements were carried out within the linear response domain adjusting the strain amplitude accordingly. The viscoelastic properties of the polymers (the storage modulus G' and the loss modulus G'') were measured in small-amplitude oscillatory shear flow as a function of time at variable temperatures and additionally under variable strain amplitude with a constant frequency ($\omega/2\pi/2\pi$ = 1 Hz), respectively.

Extrusion. A Haake Minilab (Thermo Scientific) extruder was used to extrude the polymer samples. This extruder is especially developed for the compounding of small volume samples starting from 5 g. The instrument was operated in counter rotating mode, the required extrusion time (10 min as a typical mean residence distribution time) for the mixture could be readily controlled at 200 °C. At the end of the test, the recirculation was stopped by opening the bypass valve and extruding the sample as a rod.

General Procedure of RAFT Polymerization of Styrene with DBTTC. Linear polystyrene (PS) carrying a RAFT-functionality (trithiocarbonate) in the middle of the polymer chain with various chain lengths were prepared via the following procedure: styrene (20 mL), toluene (20 mL) and dibenzyl trithiocarbonate (DBTTC) were dissolved in toluene in a 100 mL Schlenk tube and the reaction mixture was degassed by three freeze–pump–thaw cycles and left under argon. The reaction was performed at 110 °C for variable time intervals (see Table 1, e.g., 24 h). The polymerizations were stopped by cooling the reaction flask with liquid nitrogen. The individual

Table 1. Reaction Conditions Employed for the Preparation of the Initial Polymers via the RAFT Process as Well as Their Molecular Weight Characteristics

polymer	$[CTA]_0$[a] (mM)	monomer	reaction time (h)	M_n[b] (kDa)	$Đ$
1a	2.2	styrene	8	21	1.34
1b	2.2	styrene	24	51.3	1.27
1c	1.1	styrene	48	101.9	1.35
1d	0.28	styrene	26	141.7	1.72
2	0.28	styrene	24	139.2	1.68
3	23.4	*n*-butyl acrylate	0.4	2.7	1.33
4a	–	styrene	–	267	1.11
4b	–	styrene	–	70.9	1.04

[a]DBTTC (**1a**, **1b**, **1c**, **1d**, and **3**) or DoPAT (**2**) were used for the preparation mid-chain functional and chain-end functional polymers, respectively. [b]Determined via DRI detection SEC using linear PS standards.

dx.doi.org/10.1021/ma401749h | *Macromolecules* 2013, 46, 8079–8091

Scheme 2. Synthetic Strategy for the Preparation of the Linear Polystyrenes and Polyacrylates Employed in the Present Study Carrying a Trithiocarbonate Functionality in the Mid-Chain and Terminal Position

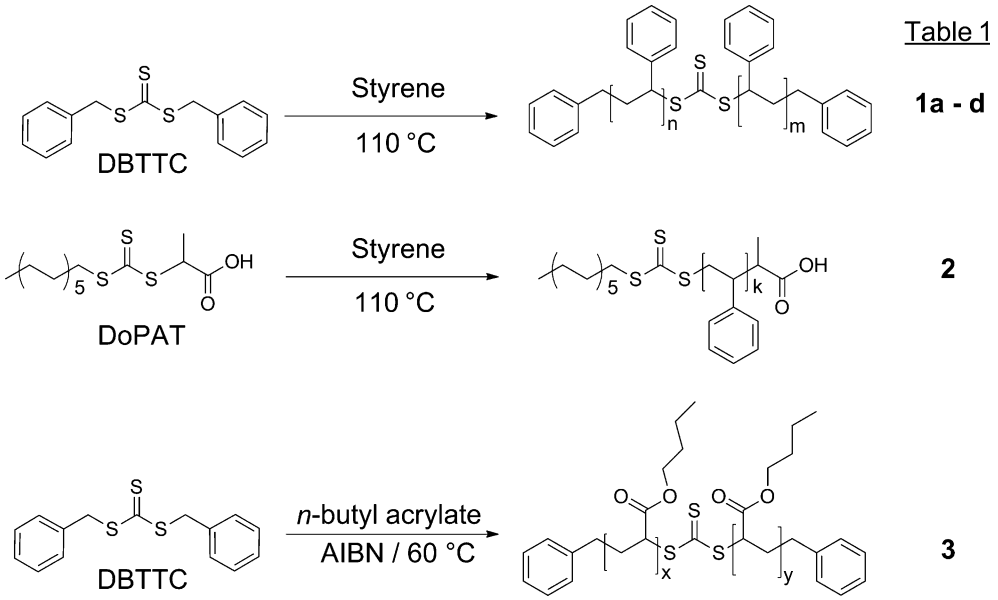

concentrations of the RAFT agent as well as the resulting polymer molecular weight properties can be found in Table 1.

General Procedure of RAFT Polymerization of Styrene with DoPAT. Linear polystyrene (PS) carrying a RAFT-functionality (trithiocarbonate) at the terminus of the polymer was prepared by the following procedure: styrene (20 mL), toluene (20 mL) and 2-((dodecylsulfanyl)carbonothioyl)sulfanyl propanoic acid (DoPAT) (0.28 mmol L^{-1}) were dissolved in toluene in a 100 mL Schlenk tube and the reaction mixture was degassed by several freeze–pump–thaw cycles and left under argon. The reaction was performed at 110 °C for 24 h. The polymerization was stopped by cooling the reaction vessel with liquid nitrogen.

General Procedure of RAFT Polymerization of n-Butyl Acrylate with DBTTC (Scheme 2). Linear *n*-butyl acrylate (P*n*BA) carrying a RAFT-functionality (trithiocarbonate) in the middle of the polymer was prepared by the following procedure: *n*-butyl acrylate (10 mL), toluene (5 mL), AIBN (6.2 mmol L^{-1}), and DBTTC (31.2 mmol L^{-1}) were dissolved in a 50 mL Schlenk tube and the reaction mixture was degassed by three freeze–pump–thaw cycles and left under argon. The reaction was performed at 60 °C for 25 min. The polymerization was stopped by cooling the reaction flask with liquid nitrogen.

Thermal Treatment. Thermal treatment of the polymers in air atmosphere were carried out in an isothermal oven set to 100, 120, 140, 160, 180, and 200 °C (±1 °C) where the polymer samples (5 mg) were kept for 24 h in open vials under air. The 10 mL Schlenk tubes for degradation under inert atmosphere were dried with a heat gun and cooled under argon. The polymer samples (each ca. 5 mg) were added into the Schlenk tube and evacuated for 60 min and left under argon. Subsequently, the thermal degradation of the samples under inert atmosphere was carried out in an oil bath at the above-noted temperatures for 24 h. The kinetic studies were conducted at variable temperatures both in air and in inert atmospheres, with the polymer samples being removed periodically at preset time intervals.

Theoretical Procedures. Quantum chemical calculations were carried out with Gaussian 09.[34] Geometry optimizations and frequency calculations were carried out using M06-2X[35,36] with Pople's basis set 6-31G(d,p)[37−39] and conformations were also fully searched at this level. M06-2X, a modern functional that is designed to model dispersion correctly, was chosen on the basis of its good performance across broader test sets of organic reactions.[35] Free energies in the gas-phase were calculated using the standard textbook formulas for the statistical thermodynamics of an ideal gas under the harmonic oscillator–rigid rotor approximation. Rate coefficients were calculated using the transition state theory in conjunction with Eckart tunnelling corrections.[40] Further details are provided in the electronic Supporting Information.

RESULTS AND DISCUSSION

RAFT polymerization of styrenes and acrylates is an ideal candidate for use in industrial applications within the controlled/living radical polymerization family due to its nondemanding reaction conditions, the frequent use of these monomers in industry and the similarity to conventional free radical polymerization processes. It is necessary to understand the stability of RAFT-made polymers under both thermal and mechanical stress to eventually allow RAFT polymers to be processed. Thus, trithiocarbonate mid-chain functional linear polystyrenes (emulating a Z-group design)[16] have been prepared via RAFT polymerization with various chain lengths. In addition—for postdegradation SEC–ESI–MS analysis—one poly(*n*-butyl acrylate) with a trithiocarbonate mid-chain function has been prepared. The resulting molecular weight distributions are depicted in Figure 1 and the relevant reaction conditions are collated in Table 1.

The stability of polymers is usually studied in inert atmospheres; however, stability in an oxygen environment is also important for real life processing conditions. Therefore, the thermal stability of trithiocarbonate mid-chain functional polystyrenes, trithiocarbonate chain-end functional polystyrenes and nonfunctional polystyrenes has been studied in both air and inert nitrogen atmospheres via time-dependent size exclusion chromatography. Specifically, samples of each type of polymer exposed to 200 °C in air atmosphere have been regularly removed from the high temperature environment and subjected to SEC analysis. Inspection of Figure 2 clearly indicates a decrease in the number-average molecular weights, M_n, of all polymers at 200 °C. The overall shape of the curves indicates that the molecular weight of the polymers significantly decreases as a function of time including for anionic polystyrene. The degradation behavior of the polymers in air displayed no dependence neither on the nature of the functional groups within them nor the synthetic route, as

dx.doi.org/10.1021/ma401749h | *Macromolecules* 2013, 46, 8079–8091

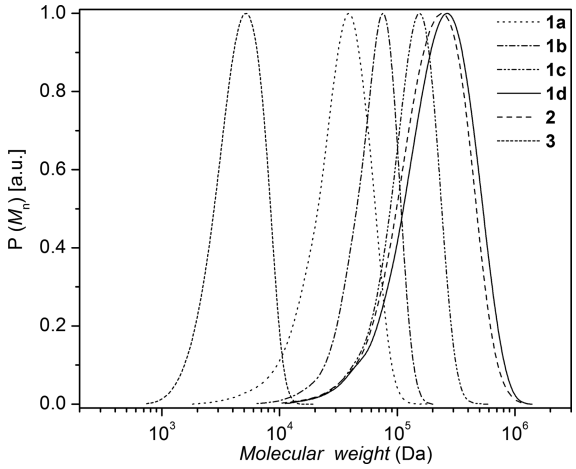

Figure 1. SEC traces of trithiocarbonate midfunctional linear polymers employed in the degradation and extrusion experiment prior to stress: **1a** ($M_{n,SEC}$ = 21 kDa, $Đ$ = 1.34), **1b** ($M_{n,SEC}$ = 51.3 kDa, $Đ$ = 1.27), **1c** ($M_{n,SEC}$ = 101.9 kDa, $Đ$ = 1.35), **1d** ($M_{n,SEC}$ = 151.7 kDa, $Đ$ = 1.72), **2** ($M_{n,SEC}$ = 139.2 kDa, $Đ$ = 1.68), **3** ($M_{n,SEC}$ = 2.7 kDa, $Đ$ = 1.33).

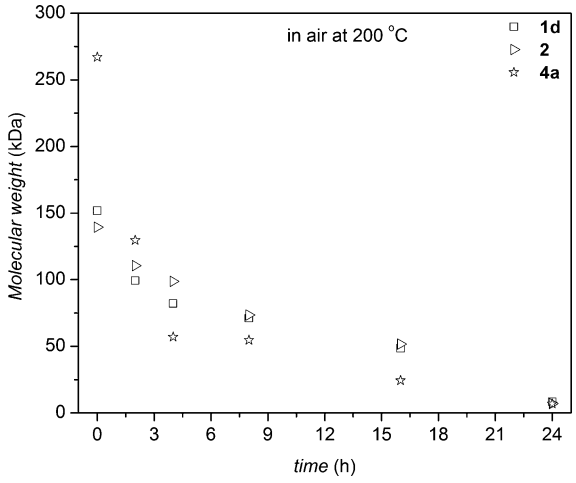

Figure 2. Decrease of the number-average molecular weight, M_n, of trithiocarbonate midfunctional polystyrene (**1d**), trithiocarbonate end-functional polystyrene (**2**), and nonfunctional polystyrene (**4a**, prepared via anionic polymerization) at 200 °C as a function of time in an air atmosphere. For the full molecular weight distributions associated with the displayed averages refer to Figure S3 in the Supporting Information.

anionically prepared polystyrene degrades in a similar way. In addition to the data displayed in Figure 2, the polymers (**1a**, **1b**, **1c**, **1d**) have been kept at various temperatures for 24 h before SEC analysis (refer to Figure S1 and Figure S2 in the Supporting Information). However, no degradation can be observed below 120 °C. At temperatures exceeding 120 °C, the polymer is above the glass transition temperature (T_g), starts to melt and its solid-state characteristics are lost. Above the T_g, the chain mobility and diffusion (oxygen, polymer etc.) is significantly enhanced, possibly allowing for accelerated degradation. Several mechanisms have been proposed in the literature for degradation of polystyrenes in air, where chain scission yields radical species.[41] When oxygen reacts with the newly formed radicals, a reactive peroxy radical intermediate can form, accelerating the radical driven chain scissions. Thus, the oxygen content is extremely relevant for the thermal degradation of the polymers under air at elevated temperatures.[42−44] However, under conditions where oxygen is present, the subtle difference in chain architecture—mid-chain vs end chain functional RAFT polymers—are of minor importance.

Since extrusion is typically conducted at high temperate and high pressure (e.g., 300 bar), the oxygen content is substantially reduced. Thus, we subsequently turned our attention to investigate the polymer stability under an inert atmosphere to determine the effect of the chain transfer agent's position on the stability behavior of the polymers. Initially, the three trithiocarbonate mid-chain functional polymers (**1b**, **1c**, **1d**) featuring different molecular weights have been kept at various temperatures for 24 h in an inert atmosphere. Subsequently, the number-average molecular weights, M_n, of the polymers have been determined via SEC, indicating that the thermal degradation becomes prominent close to 140 °C if kept for 24 h and is completed between 180 and 200 °C (refer to to Figure 3). Inspection of Figure 3 indicates that only the RAFT

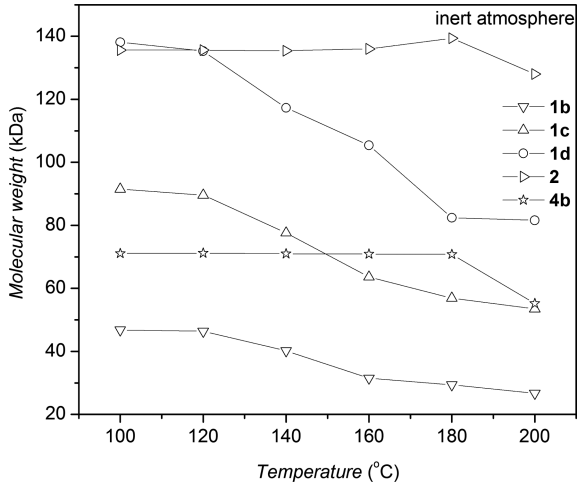

Figure 3. Number-average molecular weight, M_n, of trithiocarbonate midfunctional polystyrene (**1b**, **1c**, **1d**), trithiocarbonate end-functional polystyrene (**2**), and nonfunctional polystyrene (**4b**, prepared via anionic polymerization) kept at variable temperatures for 24 h in an argon atmosphere. The full molecular weight distributions for one sample polymer (**1c**) and polymer (**2**) can be found in Figure S5 and Figure S6 in the Supporting Information, respectively.

mid-chain functional polymers (**1b**, **c**, **d**) degrade with increasing temperature—to approximately half their initial M_n—at 200 °C within 24 h. In contrast, the trithiocarbonate chain-end functional linear polymer (**2**) and anionic linear polystyrene (**4a**)—while being treated identically—display basically no degradation, thus indicating that the mid-chain functional position of the trithiocarbonate unit is critical for the polystyrenes' stability. Such an observation becomes especially important when recalling that these polystyrenes resemble the principle design of Z-group approach prepared star and comb macromolecules. Furthermore, reductions in molecular weight of trithiocarbonate mid-chain functional polystyrenes (**1c** and **1d**) both under air and inert atmosphere during thermal treatment are depicted in Figure S4 in the Supporting Information.

In a subsequent step, the stability of the trithiocarbonate functional polymers was quantified by determining the degradation kinetics and activation energy of the thermal

dx.doi.org/10.1021/ma401749h | Macromolecules 2013, 46, 8079−8091

decomposition process. Such a kinetic analysis assists probing the degradation mechanism as well as predicting the thermal stability as a function of time of the polystyrenes in an extrusion processes. The kinetic degradation studies under inert atmosphere were carried out employing two chain lengths of the mid-chain functional RAFT polymers (**1a** and **1c**, see Table 1). The kinetics of the decomposition are investigated under isothermal conditions in the melt at different temperatures with the polymers being kept at various temperatures for preset time intervals. SEC was applied to determine the degradation kinetics of the midfunctional RAFT polymers by monitoring the number-average molecular weight after each time interval. The molecular weight of the polymers is plotted vs reaction time at different temperatures as depicted in Figure 4. Degradation rate coefficients, k_d, are obtained by fitting the $M_n(t)$ data depicted in Figure 4 to eq 1 (see below for a detailed description of fitting process). As evident from Figure 4, both polymers show increased degradation rates with increasing temperature.

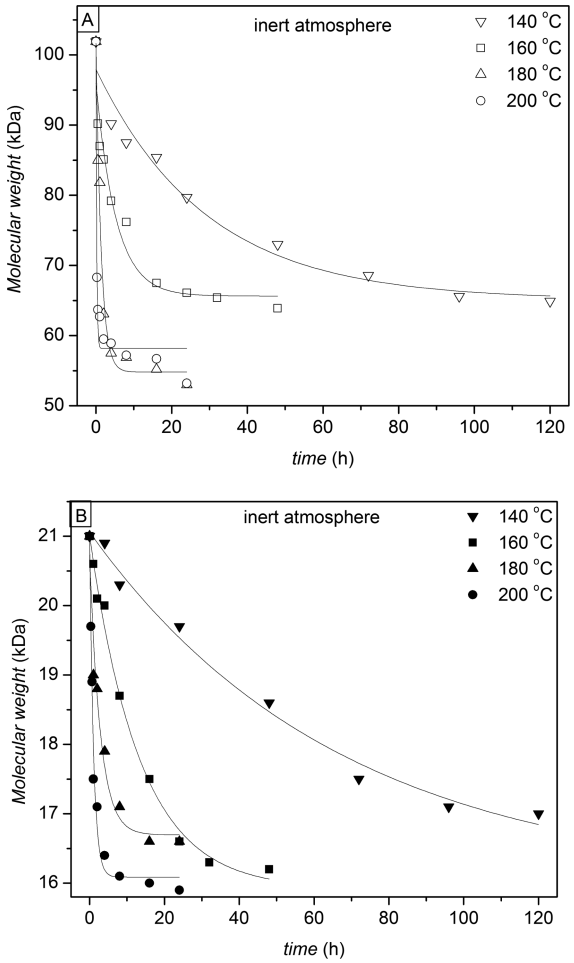

Figure 4. Number-average molecular weight, M_n, as a function of time at variable temperatures for the degradation of trithiocarbonate mid-chain functional polystyrenes featuring different initial molecular weights (polymer **1c**, $M_{n,SEC}$ = 102 kDa; $Đ$ = 1.35, at the top, A) and **1a**, $M_{n,SEC}$ = 21 kDa; $Đ$ = 1.34, at the bottom, B), see Table 1). The depicted lines represent exponential decay fits according to eq 1 to deduce the first order rate coefficient for degradation. Exemplary, the full molecular weight distribution evolution is depicted for degradation at 200 °C for both polymers in Figure S7 and S8 in the Supporting Information.

To allow for an optimum comparability of the SEC data, all SEC analyses were conducted on the same day for each degradation temperature. A discussion of the error associated with the SEC experiments can be found below. Inspection of Figure 4A—where the degradation of the high molecular weight sample is monitored—indicate that at 200 °C almost a halving of the initial M_n is observed within 8 h or a 10% reduction within 3 min. A long-term test exposing **1c** to 160 °C for up to 504 h (3 weeks) also indicated a close to halving of the molecular weight ($M_{n,SEC}^{160\ °C,\ 504\ h}$ = 49.6 kDa, $Đ$ = 1.48, refer to Figure S9). For polymer **1a**, ($M_{n,SEC}^{160\ °C,\ 504\ h}$ = 15.4 kDa, $Đ$ = 1.45, refer to Figure S10) a similar trend is observed as for **1c**, however, the molecular weight decrease is not as pronounced, an observation which is underpinned by the long-term (3 weeks) degradation that at 160 °C, too (refer to Figure S10).

The rate coefficients, k_d, (refer to Table 2) for the thermal degradation of the corresponding polymers were determined

Table 2. Rate Coefficient Data[a] for the Thermal Degradation of the Polymers 1a and 1c as Well as the Parameters Obtained from Equation 1

T/°C	ln (k_d/ s^{-1}) (**1a**)	M_n^0 (**1a**)	M_n^∞ (**1a**)	ln (k_d/ s^{-1}) (**1c**)	M_n^0 (**1c**)	M_n^∞ (**1c**)
140	−12.45	5.3	15.8	−11.56	32.8	65.1
160	−10.78	5.1	15.9	−9.86	30.3	65.3
180	−9.24	4.0	16.7	−8.51	46.8	54.8
200	−8.24	4.9	16.1	−7.23	43.4	58.15
200[b]	−7.98	4.2	16.8	−6.89	48.72	52.62

[a]Note: The units of M^0 and M^∞ are kDa. [b]Repeat run.

using the eq 1, where M_n^0 is the molecular increment added to M_n^∞ at t = 0 corresponding to the initial molecular weight of $M_n^0 + M_n^\infty$, t is the time the polymer is exposed to each temperature, $M_n(t)$ is the observed molar mass after heating for time t and M^∞ is the molar mass of the polymer at infinite time. Equation 1 was fitted—not forcing the fit through any data point (including the starting M_n value) as all data points are beset with an identical SEC error—to the data in Figure 4, parts a and b. The kinetic analysis thus demonstrates that the degradation process can be described by first order kinetics suggesting that a unimolecular scission reaction may be operational. For a further exploration of the reaction mechanism, the reader is referred to the later discussed SEC−ESI−MS analysis.

$$M_n(t) = M_n^0 e^{-k_d t} + M_n^\infty \quad (1)$$

Subsequently, $k_d(T)$ was employed to construct Arrhenius plots for each molecular weight (refer to Figure 5). Activation energies, E_a, for the thermal degradation of polymer **1a** and **1c** were deduced from the slopes of the Arrhenius plots according to eq 2, where R is the gas constant (8.314 J mol^{-1} K^{-1}), T is the temperature in Kelvin and A is the frequency prefactor.

$$k(T) = Ae^{-E_a/RT} \quad (2)$$

By plotting ln k_d against $1/T$, the slope and intercept provides $-E/R$ and ln (A), respectively. The Arrhenius analysis indicates that the activation energy does not show significant differences for different chain lengths of the mid-chain the trithiocarbonate functional polymers (115 kJ·mol^{-1} for **1a** and 116 kJ·mol^{-1} for **1c**) within experimental error in inert atmosphere. The error in

dx.doi.org/10.1021/ma401749h | Macromolecules 2013, 46, 8079−8091

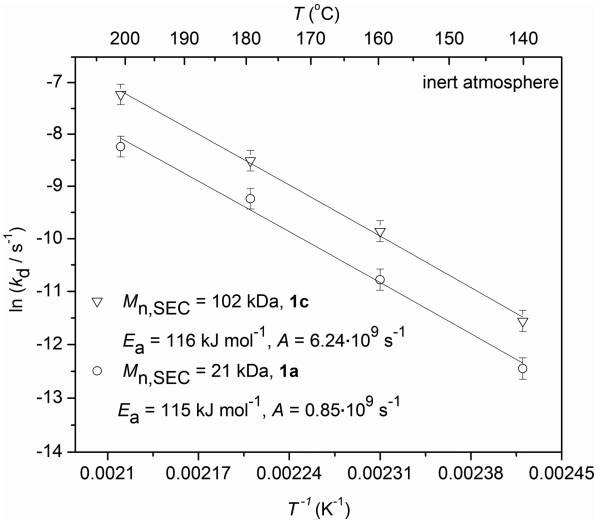

Figure 5. Arrhenius plots for the degradation of RAFT based polystyrenes of two initial molecular weights featuring a trithiocarbonate mid-chain functionality in an inert atmosphere. The error bars are deduced from repeat experiments (for details refer to the text).

each data point can be estimated by repeat experiments of the degradation of polymer **1a** and **1c** at given temperatures, e.g. 200 °C (see Figure S11 and S12 in the Supporting Information). The main component of the error is associated with the SEC analysis, which typically features uncertainties close to ± 20%. This expectation is confirmed by inspecting the repeat runs depicted in Figure S11 and S12 in the Supporting Information. The first order analysis of the repeat runs yields for **1a** at 200 °C the rate coefficient of $\ln (k_d/s^{-1})_{200\ °C} = -7.98$, while for **1c** $\ln (k_d/s^{-1})_{200\ °C} = -6.89$ are observed. Thus, the experimental error translates into an approximate error of $\ln k_d$ of close to 0.2 logarithmic units. The error is reflected in the error bars in Figure 5 (Arrhenius plots) and results in an error for E_a of close to 4 kJ mol^{-1}.

Further inspection of Figure 5 reveals that—while the activation energy is similar for both chain length—a significant difference (factor 7.3) is observed in the pre-exponential factor. Interestingly, the higher molecular weight polymer **1c** (which thus features longer chain segments on either side of the trithiocarbonyl functionality) degrades faster than polymer **1a**, having shorter chain length. While such an observation may seem surprising at first, it is not without precedent. Guimard et al. reported an entropic effect on the chain scission reaction in Diels–Alder systems, which are—while not fully identical with the present case—similar in that different chain length blocks were investigated in retro Diels–Alder reactions.[45] In that work it was shown that a large component of the chain length effects on the entropy arose in the translational and rotational components which are dominated by the mass and geometries of the polymer chains rather than the specific nature of the chemical reaction taking place between them, and hence should be equally applicable to the present reactions. On a practical level, it is important to recognize that the longer the chain length, the less thermal stress should be applied to the polymer system during processing to avoid degradation.

While the SEC analysis provides an indication that the trithiocarbonate functional polymers are cleaved by mid-chain scission at the trithiocarbonate function at elevated temperature, a more detailed molecular proof is required of the reaction mechanism. The thermal decomposition of trithiocarbonate mid-chain functional polymer—on the example of poly(*n*-butyl acrylate)—was thus investigated in the melt. Acrylate-based trithiocarbonate polymers with low molecular weight have been chosen for the chemical analysis of the degraded material, since the polyacrylates can be readily analyzed via SEC–ESI–MS. The reason for not subjecting polystyrenes to an alternative matrix-assisted laser desorption/ionization (MALDI) analysis is based on the observation that RAFT polymers—which readily absorb UV irradiation via their thiocarbonyl thio function—tend to strongly fragment upon UV-laser irradiation during the MALDI processes. Unfortunately, the polystyrenes do not lend themselves well to ESI–MS analysis due to their very poor ionizability. Initially the structural integrity before degradation of the polyacrylate **3** was established via ESI–MS analysis. A zoom mass spectrum of a repeat unit for a detailed assignment of all detected species is shown in Figure S13 in the Supporting Information. The experimental and theoretical m/z have been summarized in Table S1 for all detected species. Inspection of Figure S13 underpins that the main product is the polymer **3**, occurring as well in both double and triple charged states.

Subsequently, the chemical reactions occurring both under air and inert atmosphere during the thermal treatment of polymer **3** have been thoroughly investigated via SEC–ESI–MS. Polymer **3** was kept at 200 °C for 24 h both under air and inert atmosphere before SEC–ESI–MS analyses. The SEC–ESI–MS spectra of the corresponding samples were recorded to determine the products of the thermal degradation processes under ambient atmosphere (refer to Figure 6). In assigning these new species formed via thermal treatment in air, our attention focused on the reactivity of the trithiocarbonate mid-chain functionality and its reactions. As depicted in Figure 6a, the vinyl terminated species **3a** are formed as products of the thermal treatment. The addition of oxygen to the new vinyl terminated polymer **3a** to form an epoxide is a well-known reaction that proceeds readily at elevated temperatures in polymeric acrylic systems.[41] The formation of the double bond of polymer **3a** and the resulting epoxide **3b**—a product which commonly occurs when macromonomers are exposed to elevated temperatures in air[41]—was confirmed via the respective peak assignments (refer to Table 3 and Figure 6a). In addition to the formation of the main products **3a** and **3b**, some minor degradation products are formed, which result from follow on degradation processes and possible side chain scissions. However, due to the limited signal-to-noise ratio in the mass spectroscopy data, these have not been further assigned. Instead we focused our attention on degradation processes under an inert atmosphere, where much clearer species formation is observed (refer to Figure 6b). Under inert atmosphere, the mechanism of the decomposition is mainly via β-elimination of the trithiocarbonate groups. The most important pathway is the β-elimination of thiocarbonylthio compounds possessing a β-hydrogen, leading to the formation of unsaturated species (**3a** or **3a′**) and the corresponding acid (**3c**). When there is a hydrogen in β-position to the thiocarbonylthio moiety, the decomposition can proceed via a Chugaev-type elimination process.[46−50] The possible mechanism proposed for the decomposition of polymer **3** is depicted in Scheme 3 (under an inert atmosphere).

To further study the mechanism, *ab initio* molecular orbital calculations were conducted on small representative models of the acrylate and styrene mid-chain functional trithiocarbonates as shown in Scheme 4. It should be noted that the reactant has

dx.doi.org/10.1021/ma401749h | *Macromolecules* 2013, 46, 8079–8091

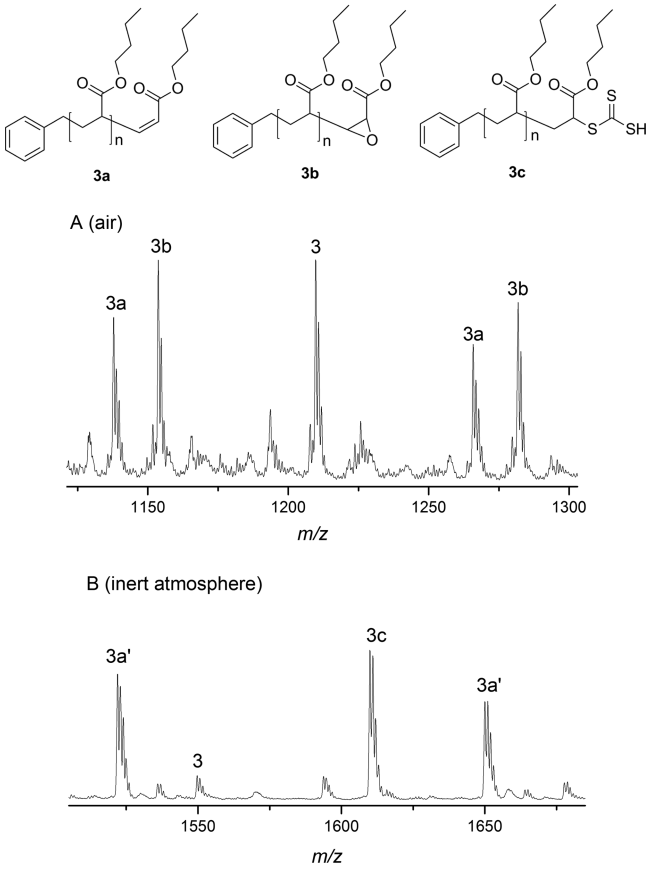

Figure 6. ESI−MS spectra of the thermally treated (200 °C, 24 h) trithiocarbonate midfunctional P*n*BA (**3**) under an air (A) and a nitrogen atmosphere (B).

Table 3. Assignment of the Observed Species in the SEC−ESI−MS Spectra of the Polyacrylate 3 after Thermal Treatment under Air and in a Nitrogen Atmosphere at 200 °C for 24 h

species	m/z_{theo} (Da)	m/z_{exp} (Da)	$\Delta m/z$
[**3** (n = 7) + Na]$^+$	1209.60	1209.39	0.21
[**3a** (n = 7) + Na]$^+$	1137.71	1137.96	0.25
[**3b** (n = 7) + Na]$^+$	1153.70	1153.13	0.57
[**3a′** (n = 10) + Na]$^+$	1521.96	1521.96	0.00
[**3c** (n = 9) + H]$^+$	1481.82	1481.75	0.07

to undergo a conformational change prior to reaction and this is taken into account in the calculations by referencing the

Scheme 4. Model Reaction Studied via *ab Initio* Quantum Chemical Calculations

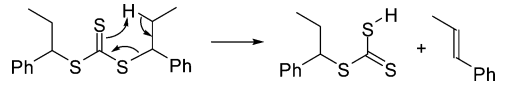

barrier on the overall energy difference between the global minimum conformation of the reactant and transition structure. The rate coefficient for this reaction was calculated over the experimental temperature range of 413−473 K in the gas phase. The Arrhenius model was subsequently fitted to the rate data to estimate an effective barrier and frequency factor for the reaction. Corrections for quantum-mechanical tunneling were included in the rate coefficients but were relatively small at this temperature (ca. a factor of 1.4) and the Arrhenius plot was reasonably linear, consistent with experiment. The Arrhenius parameters obtained in the simulation over this range are 170 kJ mol^{-1} and 1.9 × 10^{15} s^{-1} for the styrene trithioester, and 167 kJ mol^{-1} and 1.2 × 10^{12} s^{-1} for the methyl acrylate system. The results obtained are in good qualitative agreement with a previous study of this reaction in a model xanthate-based system,[51] but understandably show significant differences to the polymeric styrene system of the current work, due to the chain length (and to a lesser extent medium) effects on the entropy of reaction.[45] Thus, for the short chain model, the reaction of styrene trithiocarbonate is endergonic by 14 kJ mol^{-1} at 413 K, decreasing to just 2 kJ mol^{-1} at 473 K. For higher chain lengths, as in the polymeric system, the greater entropic driving force lowers the "debonding" temperature at which the forward reaction dominates over the reverse reaction.[45] Nonetheless, it is likely that even in the polymeric system this reverse reaction is affecting the apparent rate coefficient at lower temperatures, leading the observed rate coefficient to have a lower frequency factor and barrier compared with the small model reaction. Further details of the calculations are provided in the Supporting Information.

In a subsequent step, we proceeded to investigate the melt rheological and extrusion behavior of the synthesized polystyrenes. The polymers may undergo degradation caused by temperature in the presence of an inert atmosphere as well as additional mechanical stresses during processing. The following section first details the results from the (shear) rheology experiments. The oscillatory experiments include dynamic time sweep measurements and frequency sweep tests on predegraded and virgin polymers to probe the effects of temperature and strain on the degradation behavior of the mid-chain trithiocarbonate functional polymers. The rheological

Scheme 3. Proposed Mechanism (Shown on the Example of a Dimer Species) for the Thermal Degradation of the Trithiocarbonate Functional Polymers[a]

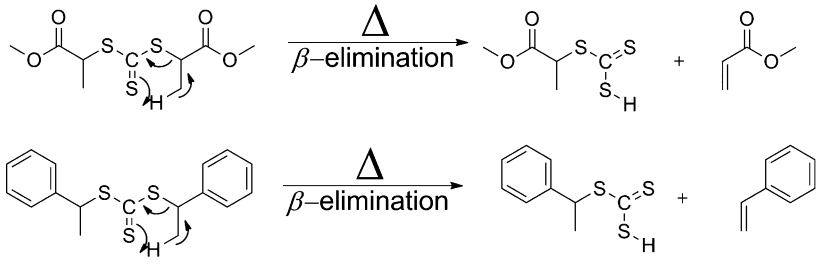

[a]The proposed Chugaev elimination is supported by the observation of species **3a′** (structurally identical to species **3a** observed in the degradation under air), and additionally by the generation of the acid **3c** (see Table 3 for the peak assignments).

dx.doi.org/10.1021/ma401749h | *Macromolecules* 2013, 46, 8079−8091

parameters storage and loss modulus ($G'(\omega,\gamma_0)$ and $G''(\omega,\gamma_0)$) in the linear and nonlinear regime are sensitive to structural changes within the polymer architectures.[32,52] Furthermore, rheological properties can be monitored continuously (e.g., several seconds) and therefore have a substantially smaller time resolution as the preparation of the samples. Additionally, one sample can be monitored throughout the degradation process. Oscillatory time sweep assessments of the polystyrene melts carrying trithiocarbonate groups in mid-chain position were additionally studied at different temperatures range from 160 to 200 °C as well as various strain amplitudes range from γ_0 = 0.01 to γ_0 = 0.2 at 180 °C.

Initially, the molecular stability of polymer **1c** (trithiocarbonate mid-chain functional polymer) and **4b** (anionically prepared nonfunctional polystyrene) was investigated and compared at 180 °C and at a frequency of $\omega/2\pi$ = 1 Hz and γ_0 = 0.1 strain. The storage (G') and loss (G'') modulus of polymer **1c** and the nonfunctional polystyrene are depicted in Figure 7. Inspection of Figure 7 indicates that the storage and

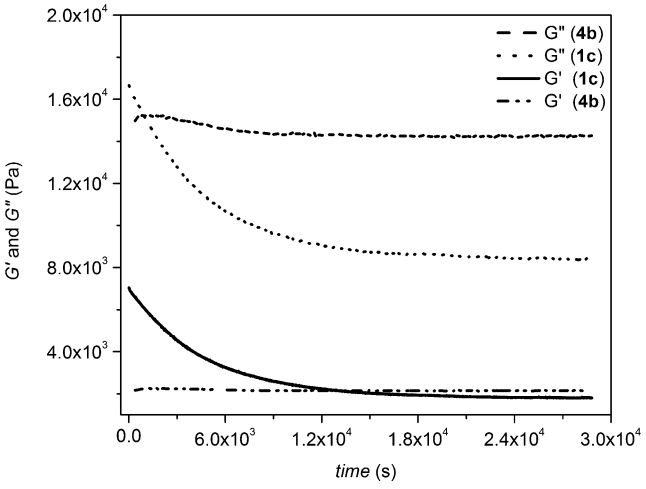

Figure 7. Comparison of the storage (G') and loss modulus (G'') as a function of time at 180 °C for polystyrene melts **1c** and **4a** at an frequency of $\omega/2\pi$ = 1 Hz and γ_0 = 0.1 strain amplitude under nitrogen atmosphere.

loss modulus of polymer **1c** decrease with increasing time at elevated temperatures in the linear regime, whereas the same rheological parameters for nonfunctional polystyrene do not vary under the same conditions. Furthermore, the ratio G''/G', which is called tan (δ), is high ($\gg$1) for liquid-like materials. Examples of tan (δ) as a function of degradation time for polystyrene **1c** and **4a** are depicted in Figure S14 in the Supporting Information. After applying both thermal and mechanical stress via the above experiment, SEC analysis revealed that the molecular weight distributions of polymer **1c** has experienced a change in molecular weight (from 102 kDa to 59.3 kDa), while the number-average molecular weight, M_n, of **4b** (70.3 kDa) stayed constant (refer to Figure S15 and S16 in the Supporting Information, respectively). The SEC results thus indicate that the trithiocarbonate mid-chain functional polymer was also degraded under these conditions, clearly detected by rheology. Moreover, the frequency sweep tests were performed at the strain of γ_0 = 10% over a frequency range from 0.01 to 15 Hz before and after the above-mentioned thermal treatment of the **1c** and **4b**, which are depicted in Figure 8 and Figure S17 in the Supporting Information,

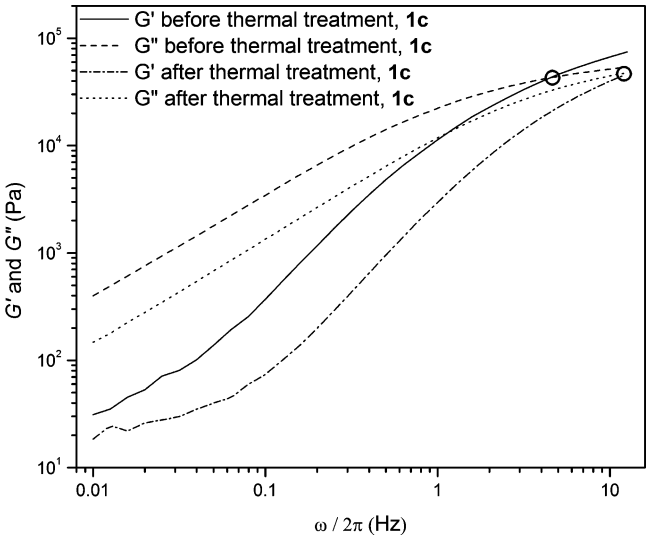

Figure 8. Comparison of the crossing point of the G' and G'' of the trithiocarbonate mid-chain functional polystyrene (**1c**) before and after the thermal treatment for 8 h at 180 °C under nitrogen atmosphere.

respectively. Inspection of Figure 8 indicates that the frequency of the crossing of G' and G'' for polystyrene **1c** shifted from 4.5 to 12.4 Hz after the thermal treatment, whereas the crossing frequencies for anionic polystyrene (**4b**) (refer to Figure S17 in the Supporting Information) were similar within the accuracy of the experiment (±10%).

It is now interesting to compare the observed reduction in molecular weight with the one predicted for **1c** for the same time period via eq 1. This prediction leads to an expectation of $M_{n,SEC}^{\ 8\ h,\ 180\ °C}$ = 55.1 kDa in conjunction with rate coefficient data collected in Table 2. The resulting M_n value after 8 h of thermal stress as well as combined thermal and mechanical stress in the linear regime result in approximately the same molecular weight within experimental error, i.e., 55.1 kDa vs 59.3k Da, respectively. Thus, it is safe to conclude that the additional mechanical stress did not result in major additional degradation of the polymeric material at 180 °C and γ_0 = 0.1 strain amplitude. Subsequently, the melt rheological behavior of polymer **1c** has been examined by dynamic time sweep tests at various amplitudes of strain in order to continuously assess the effect of the strain amplitude on the thermal degradation in the melt state. Figure S18 shows that $G'(t)$ is a function of time for different strain amplitudes, indicating that a reduction in $G'(t)$ occurs for each strain amplitude approximately at the same rate. The tan (δ) of these measurements can be found in Figure S20 in the SI section. The molecular weights of the polymers after the dynamic time sweep tests were analyzed via SEC, indicating that no additional affect of the strain amplitude on the degradation of the RAFT-based polymer exists (see Figure S19 in the Supporting Information, $M_n^{\ 8\ h,\ 180\ °C,\ 1\%\ strain}$ = 59.8 kDa, $M_n^{\ 8\ h,\ 180\ °C,\ 10\%\ strain}$ = 59.3 kDa, $M_n^{\ 8\ h,\ 180\ °C,\ 20\%\ strain}$ = 60.7 kDa) up to the limit of γ_0 = 0.2 at 180 °C for close to 8 h.

Furthermore, dynamic time sweep tests have been carried out at various elevated temperatures with a constant frequency ($\omega/2\pi$ = 1 Hz) and a constant strain amplitude (γ_0 = 0.1) to investigate the additional effects of the mechanical stress on the decomposition of the trithiocarbonate functional group compared to pure thermal degradation. Once again, the

dx.doi.org/10.1021/ma401749h | Macromolecules 2013, 46, 8079−8091

molecular weight of the samples after rheological assessment have been measured by SEC (refer to Figure 9). The molecular

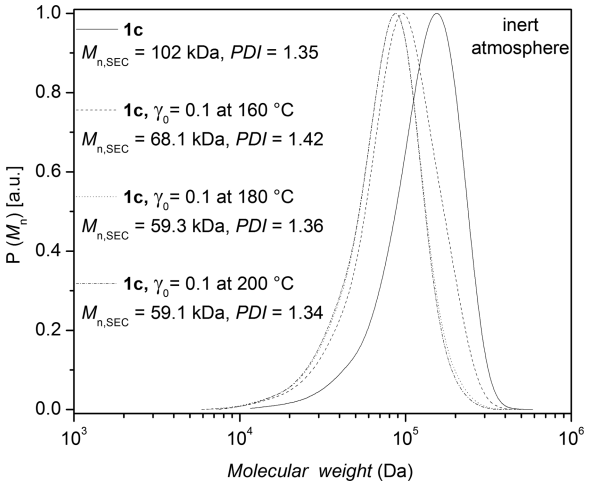

Figure 9. Comparison of number-average molecular weights of polymer **1c** at mechanical excitation at a frequency of $\omega/2\pi$ = 1 Hz in nitrogen atmosphere with a constant strain amplitude (γ_0 = 0.1) at 180 °C. SEC traces were taken after 8 h of mechanical shear.

weight of polymer **1c** decreases from 102 kDa to 76.2 kDa at 160 °C under exclusive thermal degradation (refer to Figure 4a), whereas the M_n of the polymer decrease to 68.1 kDa in the additional presence of mechanical stress at a strain amplitude (γ_0 = 0.1), suggesting there may be a minor effect of additional stress on the degradation. However, there is no additional effect of mechanical stress for temperatures exceeding 160 °C (refer to Figure 9).

In a next step, the absolute value of the complex viscosities as a function of frequency at a temperature of 180 °C before and after the dynamic time sweep test for the polymer **1c** and the anionic polystyrene **4b** are displayed in Figure 10. The dynamic viscosity before the dynamic time sweep measurement is close to 6400 Pa·s for the polymer **1c**, while it is strongly reduced to

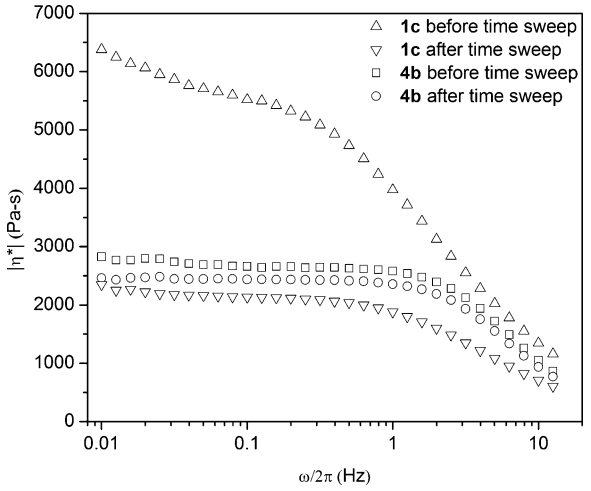

Figure 10. Comparison of the frequency depended absolute value of the complex viscosity of the trithiocarbonate functional polymer **1c** and nonfunctional polystyrene **4b** before and after dynamic time-sweep measurements (dts). The time evolution of the measurement are depicted in Figure 7.

2400 Pa·s after the measurement for the 180 °C, thus demonstrating that the viscosity was significantly lower (approximately a factor of 2.7) for polymer **1c** after the dynamic time sweep measurement due to degradation and reduction of molecular weight occurring during the mechanical measurement of the material. The anionic polystyrene **4b** displays an almost constant viscosity before and after the dynamic time sweep measurement. For a linear, monodisperse, homopolymer melt the Cox–Merz rule $|\eta^*(\omega)| = \eta(\dot{\gamma})$ can be assumed.[32,53] Moreover, the plateau viscosity is directly related to the molecular weight of the polymer. For polystyrene below the critical molecular weight M_c ($\approx 3M_e$; M_e ca. 18 kDa for polystyrene) the viscosity scales linear with M_n. For M_n larger than M_c the reptation theory describes the behavior and leads to a η_0 $M_n^{3.4}$ power dependence. The viscosity of the predegraded polymer **1c** is lower than the nonfunctional polystyrene (**4b**) and nondegraded polymer **1c**, correlated with a decrease in molecular weight of **1c** due to the applied temperature of 180 °C.

Finally, polymer processing provides a mean to shape and to manufacture plastic materials products from polymer resins or powder. This is generally achieved using extrusion or injection molding processes to form the desired shape of the end product. To mimic the extrusion process of the trithiocarbonate mid-chain functional polymer **1c** and **1d**, a 10 min residence time in the extrusion barrel—to remain consistent with the mixing average residence time typically given in extrusion—and was followed by extrusion. However, feeding of polymer **1c** and **1d** took close to 10 min, therefore the total residence time is more than 10 min at 200 °C. The change in molar mass after extrusion can provide a measure for the combined thermal and mechanical degradation. Again, the molecular weight reduction observed during extrusion can be compared to the reduction in molecular weight observed in pure thermal degradation experiments described by eq 1 for polymer **1c**. During the entire experiment the polymers were exposed to 200 °C for 20 min (see above). The resulting M_n based on eq 1 reads 65.7 kDa (using the kinetic rate coefficients provided in Table 2). The number-average molecular weight of polymer **1c** and **1d** after extrusion was determined via size exclusion chromatography to assess the change in molecular weight (refer to Figure 11). The relative values for the number-average molecular weight based on SEC before/after extrusion were found 102 vs 65 kDa and 151 vs 109 kDa (corresponding to a 36% and 27% decrease) for polymers **1c** and **1d**, respectively.[54] Comparing the number-average molecular weight obtained for **1c** via eq 1 with the value obtained for the same polymer after extrusion, it appears that the extrusion process had no additional effect on the degradation behavior than thermal stress alone. Considering all results obtained in the present study, one can conclude that extrusion times for trithiocarbonate mid-chain functional polystyrenes such as (**1c**) need to be kept below 3 min at 200 °C to achieve only a limited (10%) reduction in molecular weight as can be calculated by employing eq 1. It is important to note that the trithiocarbonate chain-end functional linear polymer (**2**) and anionic linear polystyrene (**4a**) also display 6% and 12% reduction in molecular weight after the extrusion at 200 °C after 20 min (Tables 4 and 5, see below). Thus, the degradation extent under extrusion conditions can be estimated using kinetic data obtained via heat treatment in inert atmospheres.

dx.doi.org/10.1021/ma401749h | Macromolecules 2013, 46, 8079–8091

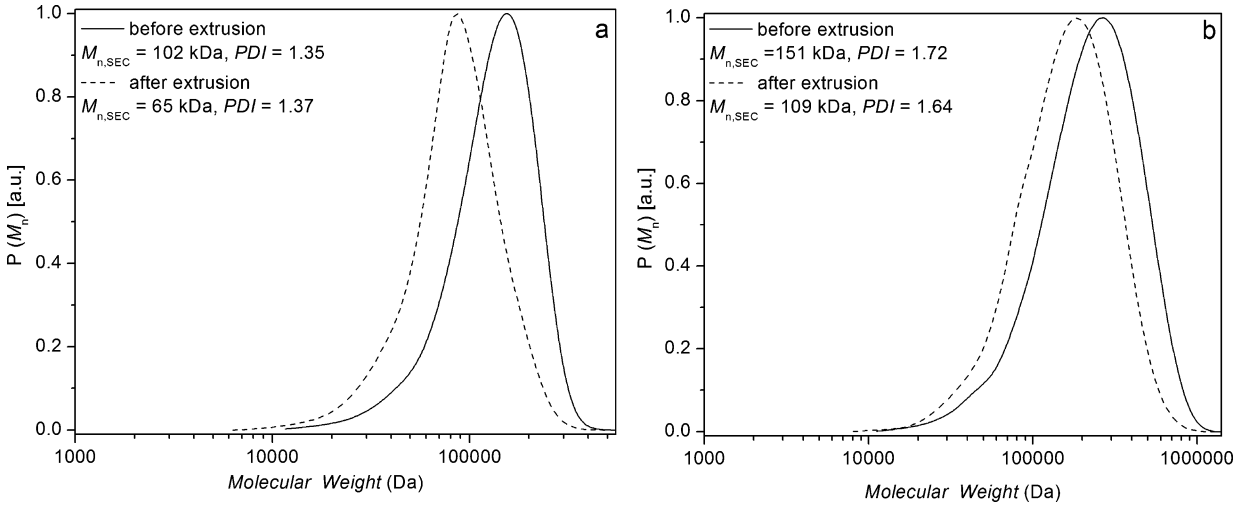

Figure 11. Comparison of the molecular weight distribution of the trithiocarbonate mid-chain functional polymer (**1c**, left side with a and **1d**, right side with b) before and after extrusion at 200 °C with a total residence time of 20 min.

Table 4. Overview Guide to Trithiocarbonate-Containing and Anionically Prepared Functional Polymer Degradation[a]

functionality	air	inert	extrusion
mid-chain	90 min (**1d**)	3 min (**1c**)	36% (**1c**)
chain-end	48 min (**1c**)	>5 h (**1c**)	6% (**2**)
anionic	15 min (**4a**)	>5 h (**4b**)	12% (**4a**)

[a]The second and third columns give the time for 10% reduction in molecular weight, M_n, at 200 °C at various conditions with different functionality. The fourth column gives the M_n reduction after 20 minutes during extrusion at 200 °C.

CONCLUSIONS

The behavior under thermal stress of trithiocarbonate mid-chain functional linear RAFT polystyrene and polyacrylates—emulating a Z-group approach macromolecular architecture—with various chain lengths was investigated in the presence of air as well as in inert atmosphere at elevated temperatures ranging from 100 to 200 °C. The thermally challenged RAFT polymers (under an inert atmosphere) were analyzed by size exclusion chromatography as a function of their exposure time to elevated temperatures. The molar mass of the trithiocarbonate mid-chain functional polymers decreased following first order kinetics at elevated temperatures, whereas there was no observable alteration in the molecular weight of trithiocarbonate end-functional polystyrene under the same conditions. First order rate coefficients for the trithiocarbonate mid-chain functional polystyrene **1a** and **1c** under inert atmosphere (E_a = 115 ± 4 kJ·mol^{-1}, A = 0.85 × 10^9 ± 1 × 10^9 s^{-1}, $M_{n,SEC}$ = 21 kDa and E_a = 116 ± 4 kJ·mol^{-1}, A = 6.24 × 10^9 ± 1 × 10^9 s^{-1}, $M_{n,SEC}$ = 102 kDa) for the thermal degradation were determined from the time dependent evolution of the number-average molecular weight. Interestingly, the degradation rate was found to be a function of the polymer chain length, which is potentially attributable to an entropic effect. The decomposition mechanism of the mid-chain functional RAFT polymers possessing an β-hydrogen most likely proceeds according to a Chugaev-type elimination. Further, rheological experiments indicate that there is no additional effect of the degradation on the thiocarbonylthio functionality under mechanical stress at elevated temperatures under inert atmosphere up to γ_0 = 0.1. The trithiocarbonate mid-chain functional polymers placed under mechanical stress showed a similar degradation behavior with respect to their molecular weight as a function of time under inert atmosphere. In addition, SEC traces recorded after extrusion for 20 min under inert atmosphere demonstrated that the number-average molecular weight of the thiocarbonylthio mid-chain functional polymers decrease between 27% and 36% at elevated temperatures close to 200 °C, depending on the polymer chain length and that—also during extrusion—mechanical stress does not lead to elevated degradation rates. The present work not only provides fundamental knowledge on the thermal decomposition mechanisms and kinetics for trithiocarbonate mid-chain functional polymers in the melt, but additionally suggests that Z-group designed materials can be processed via melt extrusion at elevated temperature provided the extrusion times are on average below 3 min at 200 °C or 22 min at 180 °C leading to an acceptable 10% of cleaved chains. Acceptable degradation rates during processing can—on the basis of the herein provided kinetic data eq 1—be predetermined. An

Table 5. Final values of M_n reached at long reaction time (24 h) for all investigated polymer samples at 200 °C in air and inert atmosphere environments

functionality	air	inert
mid-chain	M_n (t = 0) = 102 kDa (**1c**)	M_n (t = 0) = 102 kDa, (**1c**)
	M_n (t = 24 h) = 9 kDa	M_n (t = 24 h) = 53 kDa
chain-end	M_n (t = 0) = 140 kDa (**2**)	M_n (t = 0) = 140 kDa (**2**)
	M_n (t = 24 h) = 7 kDa	M_n (t = 24 h) = 128 kDa
anionic	M_n (t = 0) = 267 kDa (**4a**)	M_n (t = 0) = 71 kDa (**4b**)
	M_n (t = 24 h) = 7 kDa	M_n (t = 24 h) = 55 kDa

dx.doi.org/10.1021/ma401749h | Macromolecules 2013, 46, 8079−8091

overview guide to the degradation profiles of the studied polymers is provided in Tables 4 and 5.

■ ASSOCIATED CONTENT

Supporting Information

Further analytical data of the corresponding polymers such as a depiction of the RAFT R- vs Z-group design, molecular weight decrease as a function of temperature for 24 h under air for polymer species **1a−d**, comparison of the average number molecular weight evolution as a function of time for polymer **1c,d** under air and an inert atmosphere at 200 °C, full SEC traces of polymers **1a,c** and **2** after variable times under thermal stress, repeat experiments for the deduction of the experimental error reported in Figure 5, molecular weight evolution for long-term degradation experiments (3 weeks), supporting SEC data for the rheological experiments, and supporting data for the quantum-mechanical calculations as well as additional SEC−ESI−MS spectra. This material is available free of charge via the Internet at http://pubs.acs.org/.

■ AUTHOR INFORMATION

Corresponding Authors

*E-mail: manfred.wilhelm@kit.edu. Telephone: +49 721 608 43150 (M.W.).

*E-mail christopher.barner-kowollik@kit.edu. Telephone: +49 721 608 45641 (C.B.-K.).

Notes

The authors declare no competing financial interest.

■ ACKNOWLEDGMENTS

C.B.-K and M.W. gratefully acknowledge financial support from the German Research Council (DFG). M.L.C gratefully acknowledges generous allocations of supercomputing time from the Australian National Computing Facility, financial support from the Australian Research Council (ARC) Centre of Excellence for Free-radical Chemistry and Biotechnology and an ARC Future Fellowship. C.B.-K. acknowledges additional funding from the Karlsruhe Institute of Technology (KIT) in the context of the Helmholtz programs. The authors thank Dr. Anja Goldman (KIT), Dr. Nico Dingenouts (KIT), Alexander Haehnel (KIT), Hojjat Mahi (KIT), and Dr. Christopher Klein (KIT) for helpful discussions.

■ REFERENCES

(1) Braunecker, W. A.; Matyjaszewski, K. *Prog. Polym. Sci.* **2007**, *32*, 93−146.

(2) Roland, A. I.; Schmidt-Naake, G. *J. Anal. Appl. Pyrolysis* **2001**, *58*, 143−154.

(3) Wang, J. S.; Matyjaszewski, K. *J. Am. Chem. Soc.* **1995**, *117*, 5614−5615.

(4) Matyjaszewski, K.; Xia, J. *Chem. Rev.* **2001**, *101*, 2921−2990.

(5) Percec, V.; Barboiu, B. *Macromolecules* **1995**, *28*, 7970−7972.

(6) Haddleton, D. M.; Crossman, M. C.; Dana, B. H.; Duncalf, D. J.; Heming, A. M.; Kukulj, D.; Shooter, A. J. *Macromolecules* **1999**, *32*, 2110−2119.

(7) Hawker, C. J. *Angew. Chem., Int. Ed.* **1995**, *34*, 1456−1459.

(8) Hawker, C. J.; Bosman, A. W.; Harth, E. *Chem. Rev.* **2001**, *101*, 3661−3688.

(9) Mayadunne, R. T. A.; Rizzardo, E.; Chiefari, J.; Chong, Y. K.; Moad, G.; Thang, S. H. *Macromolecules* **1999**, *32*, 6977−6980.

(10) Barner-Kowollik, Davis, T. P.; Heuts, J. P. A.; Stenzel, M. H.; Vana, P.; Whittaker, M. *J. Polym. Sci., Part A: Polym. Chem.* **2003**, *41*, 365−375.

(11) Barner-Kowollik, C.; Buback, M.; Charleux, B.; Coote, M. L.; Drache, M.; Fukuda, T.; Goto, A.; Klumperman, B.; Lowe, A. B.; Mcleary, J. B.; Moad, G.; Monteiro, M. J.; Sanderson, R. D.; Tonge, M. P.; Vana, P. *J. Polym. Sci., Part A: Polym. Chem* **2006**, *44*, 5809−5831.

(12) Willcock, H.; O'Reilly, R. K. *Polym. Chem* **2010**, *1*, 149−157.

(13) *Handbook of RAFT-Polymerization*; Barner-Kowollik, C., Ed.; Wiley-VCH: Weinheim, Germany, 2008.

(14) Kaiser, A.; Brandau, S.; Klimpel, M.; Barner-Kowollik, C. *Macromol. Rapid Commun.* **2010**, *31*, 1616−1621.

(15) Barner-Kowollik, C.; Perrier, S. *J. Polym. Sci., Part A: Polym. Chem.* **2008**, *46*, 5715−5723.

(16) Barner, L.; Davis, T. P.; Stenzel, M. H.; Barner-Kowollik, C. *Macromol. Rapid Commun.* **2007**, *28*, 539−559.

(17) Chaffey-Millar, H.; Stenzel, M. H.; Davis, T. P.; Coote, M. L.; Barner-Kowollik, C. *Macromolecules* **2006**, *39*, 6406−6419.

(18) Boyer, C.; Bulmus, V.; Davis, T. P.; Ladmiral, V.; Liu, J.; Perrier, S. *Chem. Rev.* **2009**, *109*, 5402−5436.

(19) Favier, A.; Charreyre, M. *Macromol. Rapid Commun.* **2006**, *27*, 653−692.

(20) Dürr, C. J.; Hlalele, L.; Kaiser, A.; Brandau, S.; Barner-Kowollik, C. *Macromolecules* **2013**, *46*, 49−62.

(21) Inglis, A. J.; Sinnwell, S.; Davis, T. P.; Barner-Kowollik, C.; Stenzel, M. H. *Macromolecules* **2008**, *41*, 4120−4126.

(22) (a) Gondi, S. R.; Vogt, A. P.; Sumerlin, B. S. *Macromolecules* **2007**, *40*, 474−481. (b) Li, H.; Li, M.; Yu, X.; Bapat, A. P.; Sumerlin, B. S. *Polym. Chem.* **2011**, *2*, 1531−1535.

(23) Inglis, A. J.; Sinnwell, S.; Martina, H.; Stenzel, M. H.; Barner-Kowollik, C. *Angew. Chem., Int. Ed.* **2009**, *48*, 2411−2414.

(24) Glassner, M.; Oehlenschlaeger, K. K.; Gruendling, T.; Barner-Kowollik, C. *Macromolecules* **2011**, *44*, 4681−4689.

(25) Kempf, M.; Ahirwal, D.; Cziep, M.; Wilhelm, M. *Macromolecules* **2013**, *46*, 4978−4994.

(26) Kempf, M.; Barroso, V. C.; Wilhelm, M. *Macromol. Rapid Commun.* **2010**, *31*, 2140−2145.

(27) Castignolles, P.; Graf, R.; Parkinson, M.; Wilhelm, M.; Gaborieau, M. *Polymer* **2009**, *50*, 2373−2383.

(28) de Gennes, P. G. *Scaling Concepts in Polymer Physics*; Cornell University Press: London, 1979.

(29) Strazielle, C.; Benoit, H. O.; Vogl, O. *Eur. Polym. J.* **1978**, *14*, 331−334.

(30) Penzel, E.; Götz, N. *Angew. Makromol. Chem.* **1990**, *178*, 191−200.

(31) Gruendling, T.; Guilhaus, M.; Barner-Kowollik, C. *Anal. Chem.* **2008**, *80*, 6915−6927.

(32) Shaw, M. T. *Introduction to Polymer Rheology*; John Wiley & Sons: Hoboken, NJ, 2012.

(33) Larson, R. G. *The Structure and Rheology of Complex Fluids*; Oxford University Press: New York, 1999.

(34) Frisch, M. J.; Trucks, G. W.; Schlegel, H. B.; Scuseria, G. E.; Robb, M. A.; Cheeseman, J. R.; Scalmani, G.; Barone, V.; Mennucci, B.; Petersson, G. A.; Nakatsuji, H.; Caricato, M.; Li, X.; Hratchian, H. P.; Izmaylov, A. F.; Bloino, J.; Zheng, G.; Sonnenberg, J. L.; Hada, M.; Ehara, M.; Toyota, K.; Fukuda, R.; Hasegawa, J.; Ishida, M.; Nakajima, T.; Honda, Y.; Kitao, O.; Nakai, H.; Vreven, T.; Montgomery, J.; Peralta, J. E.; Ogliaro, F.; Bearpark, M.; Heyd, J. J.; Brothers, E.; Kudin, K. N.; Staroverov, V. N.; Kobayashi, R.; Normand, J.; Raghavachari, K.; Rendell, A.; Burant, J. C.; Iyengar, S. S.; Tomasi, J.; Cossi, M.; Rega, N.; Millam, J. M.; Klene, M.; Knox, J. E.; Cross, J. B.; Bakken, V.; Adamo, C.; Jaramillo, J.; Gomperts, R.; Stratmann, R. E.; Yazyev, O.; Austin, A. J.; Cammi, R.; Pomelli, C.; Ochterski, J. W.; Martin, R. L.; Morokuma, K.; Zakrzewski, V. G.; Voth, G. A.; Salvador, P.; Dannenberg, J. J.; Dapprich, S.; Daniels, A. D.; Farkas, Ö.; Foresman, J. B.; Ortiz, J. V.; Cioslowski, J.; Fox, D. J. *Gaussian 09, Revision C.01*; Gaussian Inc.: Wallingford CT, 2009.

(35) Zhao, Y.; Truhlar, D. G. *Theor. Chem. Acc.* **2008**, *120*, 215−241.

(36) Zhao, Y.; Truhlar, D. G. *Acc. Chem. Res.* **2008**, *41*, 157−167.

(37) Ditchfield, R.; Hehre, W. J.; Pople, J. A. *J. Chem. Phys.* **1971**, *54*, 724−728.

(38) Hehre, W. J.; Ditchfield, R.; Pople, J. A. *J. Chem. Phys.* **1972**, *56*, 2257−2261.
(39) Hariharan, P. C.; Pople, J. A. *Theor. Chem. Acc.* **1973**, *28*, 213−222.
(40) Coote, M. L.; Collins, M. A.; Radom, L. *Mol. Phys.* **2003**, *101*, 1329−1338.
(41) Bennet, F.; Lovestead, T. M.; Barker, P. J.; Stenzel, M. H.; Davis, T. P.; Barner- Kowollik, C. *Macromol. Rapid Commun.* **2007**, *28*, 1593−1600.
(42) Gruendling, T.; Weidner, S.; Falkenhagen, J.; Barner-Kowollik, C. *Polym. Chem.* **2010**, *1*, 599−617.
(43) Luo, G.; Marginean, I.; Vertes, A. *Anal. Chem.* **2002**, *74*, 6185−6190.
(44) Jiang, X.; Schoenmakers, P. J.; van Dongen, J. L. J.; Lou, X.; Lima, V.; Brokken-Zijp, J. *Anal. Chem.* **2004**, *75*, 5517−5524.
(45) Guimard, N. K.; Ho, J.; Brandt, J.; Lin, C. Y.; Namazian, M.; Mueller, J. O.; Oehlenschlager, K. K.; Hilf, S.; Lederer, A.; Schmidt, F. G.; Coote, M.; Barner- Kowollik, C. *Chem. Sci.* **2013**, *4*, 2752−2759.
(46) Chugaev, L. *Ber. Dtsch. Chem. Ges.* **1899**, *32*, 3332.
(47) Alexander, E. R.; Mudrak, A. *J. Am. Chem. Soc.* **1950**, *72*, 3194−3198.
(48) Legge, T. M.; Slark, A. T.; Perrier, S. *J. Polym. Sci., Part A: Polym. Chem.* **2006**, *44*, 6980−6987.
(49) Liu, Y.; He, J.; Xu, J.; Fan, D.; Tang, W.; Yang, Y. *Macromolecules* **2005**, *38*, 10332−10335.
(50) Zhou, Y.; He, J.; Li, C.; Hong, L.; Yang, Y. *Macromolecules* **2011**, *44*, 8446−8457.
(51) Akhtar, J.; Afzaal, M.; Vincent, M. A.; Burton, N. A.; Hillier, I. H.; O'Brien, P. *Chem. Commun.* **2011**, *47*, 1991−1993.
(52) Hyun, K.; Wilhelm, M. *Macromolecules* **2009**, *42*, 411−422.
(53) *Rheology: Principles, Measurements, And Applications*; Macosko, C. W. Wiley-VCH: Weinheim, Germany, 1994.
(54) Wiggins, K. M.; Syrett, J. A.; Haddleton, D. M.; Bielawski, C. W. *J. Am. Chem. Soc.* **2011**, *133*, 7180−7189.

■ NOTE ADDED AFTER ASAP PUBLICATION

This paper was published on the Web on October 7, 2013, with an error in Scheme 2 and the caption for Table 2. The corrected version was reposted on October 8, 2013.